Conserved Aspartic Acid 714 in Transmembrane Segment 8 of the ZntA Subgroup of P_{1B}-Type ATPases Is a Metal-Binding Residue†

Sabari J. Dutta, Junbo Liu, Zhanjun Hou, and Bharati Mitra*

Department of Biochemistry and Molecular Biology, School of Medicine, Wayne State University, Detroit, Michigan 48201

Received November 17, 2005; Revised Manuscript Received February 16, 2006

ABSTRACT: ZntA from *Escherichia coli* is a member of the P_{1B}-type ATPase family that confers resistance specifically to Pb^{2+}, Zn^{2+}, and Cd^2 salts by active efflux across the cytoplasmic membrane. P_{1B}-type ATPases are important for homeostasis of metal ions such as Cu^+, Ag^+, Pb^{2+}, Zn^{2+}, Cd^{2+} Cu^{2+}, and Co^{2+}, with different subgroups showing specificity for different metal ions. Sequence alignments of P_{1B}-type ATPases show that ZntA and close homologues have a strictly conserved Asp714 in the eighth transmembrane domain that is not conserved in other subgroups of P_{1B}-type ATPases. However, in the sarcoplasmic reticulum Ca^{2+}-ATPase, a structurally characterized P-type ATPase, the residue corresponding to Asp714 is a metal-binding residue. Four site-specific mutants at Asp714, D714E, D714H, D714A, and D714P, were characterized. A comparison of their metal-binding affinity with that of *wt*ZntA revealed that Asp714 is a ligand for the metal ion in the transmembrane site. Thus, Asp714 is one of the residues that determine metal ion specificity in ZntA homologues. All four substitutions at Asp714 in ZntA resulted in complete loss of in vivo resistance activity and complete or large reductions in ATPase activity, though D714E and D714H retained the ability to bind metal ions with high affinity at the transmembrane site. Thus, the ability to bind metal ions with high affinity did not correlate with high activity. The metal-binding affinity of the N-terminal site remained unchanged in all four mutants. The affinities of the two metal-binding sites in *wt*ZntA determined in this study are similar to values reported previously for the individual sites in isolated ZntA fragments.

P-type ATPases, a family of ATP-dependent cation transporters, have been divided into five groups depending on the specificity of the transported cation (*1*, *2*). Three of these groups, P_1-, P_2-, and P_3-type ATPases, are known to transport metal ions. A subgroup of the P_1-type group, the P_{1B}-type ATPases, transports soft metal ions such as Cu^+, Cu^{2+}, Ag^+, Zn^{2+}, Cd^{2+}, Pb^{2+}, and Co^{2+} (*3*−*14*). P_{1B}-type ATPases carry out the important task of maintaining cellular homeostasis of essential metals such as copper, cobalt, and zinc; for example, the two human copper-transporting ATPases, the Menkes and the Wilson disease-associated proteins, transport copper across membranes (*4*−*6*). P_{1B}-type ATPases are also important in mediating resistance to toxic metal ions, such as Pb^{2+}, Cd^{2+}, and Ag^+, by ATP-dependent efflux; an example is ZntA from *Escherichia coli*, which confers resistance specifically to Pb^{2+}, Zn^{2+}, and Cd^{2+} by active efflux of these metal ions out of the cytoplasm (*8*, *9*).

All P-type ATPases have a large hydrophilic loop that contains consensus domains for ATP binding and hydrolysis and a conserved aspartate residue that is phosphorylated during the catalytic cycle. Features common specifically to P_{1B}-type ATPases include a single polypeptide chain with eight transmembrane domains. In addition, most P_{1B}-type ATPases have a distinctive hydrophilic segment containing single or multiple copies of a metal-binding motif, at either the N- or the C-terminus. This motif is typically GM(T,D)-CXXC or (M,H)XXMDH(S,G)XM (*14*). The sixth transmembrane domain of all P_{1B}-type ATPases also contains the conserved (C,S,T)P(C,H) motif; the residues flanking the invariant proline are necessary for overall activity (*15*−*17*) and provide ligands to the metal ion in the transmembrane cation-binding site (*18*).

The metal-binding site(s) in the N-terminal domain of P_{1B}-type ATPases has (have) been studied for a number of proteins. NMR structural analyses of these domains from the Menkes protein, the Wilson protein, and ZntA from *E. coli* show that these domains all have the same overall $\beta\alpha\beta\beta\alpha\beta$ fold (*19*−*21*). However, the ligands and binding geometry are different for different metal ions. The N-terminal metal-binding sites in the Menkes and Wilson proteins bind Cu^+ and Ag^+ with a linear geometry with the two cysteine residues of the GMT**C**XX**C** motif providing ligands (*19*, *22*). On the other hand, the N-terminal domain of ZntA binds Zn^{2+} with tetrahedral coordination; sulfur atoms from the two cysteine residues and oxygen atoms from the aspartate residue of the GM**DC**AA**C** motif provide ligands (*20*). Thus, while Cu^+ is coordinated in a linear geometry with only two sulfurs, Zn^{2+} and likely Cd^{2+} bind with tetrahedral geometry and appear to require an additional acidic residue, which supplies one or two ligands to the metal ion. Though there is not yet any structural data for the binding of Pb^{2+} to ZntA, recent spectroscopic and mutagenesis studies indicate that binding of Pb^{2+} to the N-terminal

† This work was supported by U.S. Public Health Service Grant GM-61689 (to B.M.). S.J.D. acknowledges financial support from an American Heart Association postdoctoral fellowship.

* To whom correspondence should be addressed. E-mail: bmitra@med.wayne.edu. Phone: (313) 577-0040. Fax: (313) 577-2765.

10.1021/bi0523456 CCC: $33.50 © 2006 American Chemical Society
Published on Web 04/12/2006

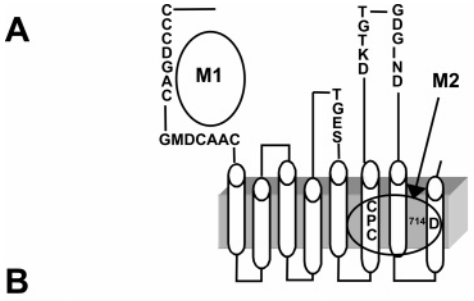

FIGURE 1: (A) Schematic representation of ZntA showing the location of the two metal-binding sites, M1 and M2, in the N-terminal domain and in the transmembrane domain, respectively. The cylinders represent the eight transmembrane domains. The positions of the CPC motif and Asp714 are indicated. (B) Sequence alignment of TM7 (M5) and TM8 (M6) in P_{1B} (P_2 and P_3) ATPases, showing the conserved Asp in the ZntA homologues. The sequences are as follows: SERCA1, the Ca^{2+}-ATPase from sarcoplasmic reticulum; the Na^+/K^+-ATPase from rat; the H^+/K^+-ATPase from rat; SaCadA, a ZntA homologue from *Staphylococcus aureus* TN554, AtHMA2, and AtHMA3, ZntA homologues from *Arabidopsis thaliana*; LmCadA, a ZntA homologue from *Listeria monocytogenes*; StZntA, a ZntA homologue from *Salmonella typhimurium*; and EcZntA, ZntA from *E. coli*.

domain of ZntA requires both the GMDCAAC motif and the upstream CCCDGAC motif and may involve at least three cysteines (Figure 1) (*23*, *24*). A consensus of this latter motif, CCX(D,E)XXC, is conserved in close homologues of ZntA. These results show that, despite the sequence homology present in the N-terminal domains of Ag^+, Cu^+, Zn^{2+}, Cd^{2+}, and Pb^{2+} transporting P_{1B}-type ATPases and the overall similarity in protein structure, the metal-binding sites have different ligands and geometry.

In contrast to the N-terminal domain, the metal-binding site in the transmembrane region of P_{1B}-type ATPases has not been extensively studied; no structural data for this site are available to date. Recent work showed that there is a single metal ion binding site in the transmembrane region of ZntA (*18*). Mutagenesis and direct metal-binding studies have demonstrated that the cysteine residues of the **C**P**C** motif provide ligands to the metal ion (*18*); however, the binding geometry or involvement of other ligands to the metal ion is not known. In addition to the N-terminal site, the transmembrane site in ZntA also determines specificity of the transported metal ion, since mutants of ZntA lacking the N-terminal domain or with a disrupted N-terminal metal-binding site have the same metal specificity and selectivity as full-length ZntA (*18*, *25*).

P_{1B}-type ATPases have been divided into six different subgroups on the basis of sequence alignment and/or putative metal ion selectivity (*26*); these subgroups are specific for $Zn^{2+}/Pb^{2+}/Cd^{2+}$ (ZntA homologues), Cu^+/Ag^+, Cu^{2+}, Co^{2+}, and as yet unassigned metal ions. These different subgroups have distinct patterns of conserved residues in the transmembrane domains, which may be responsible for metal selectivity directly by providing ligands for the most optimal metal-binding geometry or indirectly through affecting the positions of the primary metal ligands. A sequence alignment of the region in ZntA homologues comprising transmembrane domains 7 and 8 shows that an aspartate residue is strictly conserved in the middle of the eighth transmembrane domain in ZntA (Figure 1). Though this aspartate residue is invariant in ZntA homologues, it is not conserved in any other subgroup of P_{1B}-type ATPases, including the Cu^+/Ag^+, Cu^{2+}, or Co^{2+}-transporting ones. Interestingly, this aspartate residue is strictly conserved in transmembrane helix 6 of P_2- and P_3-type ATPases, which corresponds to helix 8 in P_{1B}-type ATPases. In SERCA1 from sarcoplasmic reticulum, a P_{2A}-type ATPase, this invariant aspartate, Asp800, is essential for activity (*27*, *28*). This is also true for the P_{2C}-type ATPases, for example, Na^+/K^+-ATPase from sheep kidney and the rat gastric H^+/K^+-ATPase, where mutagenesis of the corresponding Asp808 and Asp826 residues results in completely inactive enzymes (*29*, *30*). The aspartate residue is also invariant in the P_3-type yeast plasma membrane H^+-ATPases (*31*). In SERCA1, X-ray studies have shown that the asparate acts as a bridging ligand to both Ca^{2+} ions in the membrane (*32*). However, in the plasma membrane proton pumps, the aspartate appears to play a role in the conformational change of the pump during catalysis (*31*).

In this work, we examined the function of the conserved aspartate residue in the ZntA subgroup. Since the N-terminal metal-binding site in the ZntA homologues has an acidic residue as ligand, and also from analogy to SERCA1, it was likely that Asp714 is a ligand to the metal ion in ZntA. By characterizing the mutants D714E, D714H, D714A, and D714P, we show that Asp714 is essential for overall activity and that it coordinates metal ions in the transmembrane site. Thus, Asp714 is one of the residues that determine metal specificity for the ZntA subgroup of P_{1B}-type ATPases.

EXPERIMENTAL PROCEDURES

*Materials.*Buffers and water used in the metal-binding experiments were passed through Chelex 100 (Sigma) to remove extraneous metal salts and deoxygenated by flushing with argon; the estimated final metal content of buffers was <50 nM. Mag-fura-2 was from Molecular Probes. Metal standard solutions were from Sigma. Oligonucleotides were purchased from Integrated DNA Technologies, Coralville, IA.

Methods.Construction of the D714A, D714E, D714H, and D714P Mutants. All four mutants were generated using the QuickChange site-directed mutagenesis kit (Stratagene) and the following oligonucleotides: D714A, 5′ G CTG GCA GTG CTA GCA G**CG** ACG GGG GCG 3′ and 5′ CGC CCC CGT **CG**C TGC TAG CAC TGC CAG C 3′; D714E, 5′ G CTG GCA GTG CTA GCA GA**A** ACG GGG GCG 3′ and 5′ CGC CCC CGT **T**TC TGC TAG CAC TGC CAG C 3′; D714H, 5′ G CTG GCA GTG CTA GCA **C**AT ACG GGG GCG 3′ and 5′ CGC CCC CGT AT**G** TGC TAG CAC TGC CAG C 3′; D714P, 5′ G CTG GCA GTG CTA GCA **CC**T ACG GGG GCG 3′ and 5′ CGC CCC CGT A**GG** TGC TAG CAC TGC CAG C 3′. The altered bases for the mutations are indicated in boldface. In addition, a silent base change (underlined base in the oligonucleotides) was used to create a *Nhe*I or *Ace*II restriction site for rapid identification of the desired mutation. The entire sequence of the mutant genes

was verified by automated DNA sequencing (Wayne State University). The mutant genes were cloned in the pBAD/*Myc*-His C or pBAD/*Myc*-His A vector (Invitrogen) and expressed in strain LMG194(*zntA*::*cat*) as previously described for ZntA (*23*, *33*). The expression levels of all four mutants were similar to that of *wt*ZntA.

Sensitivity to Metal Salts. The sensitivity of LMG194 and LMG194(*zntA*::*cat*) in which the entire *zntA* gene is deleted, as well as LMG194(*zntA*::*cat*) transformed with plasmids containing *wt*ZntA and the individual mutants at Asp714, to metal salts was measured in a basal salts medium, pH 7.5, from which zinc salts were omitted (*34*). Cells were grown overnight and then diluted 50-fold in the same medium containing lead acetate, zinc chloride, or cadmium chloride at different concentrations. Cell growth at 37 °C was monitored by measuring the absorbance at 600 nm.

Purification of wtZntA and Asp714 Mutants. When the proteins are expressed in pBAD/*Myc* His C, they are created with a histidyl tag at the carboxy terminus. The His-tagged proteins were expressed in LMG194(*zntA*::*cat*) and purified as described earlier using Ni^{2+} chromatography and used for ATP hydrolysis and acyl phosphate formation assays (*33*).

For metal-binding studies, *wt*ZntA and the mutants at Asp714 were expressed in the pBAD/*Myc* His A vector (Invitrogen) in strain LMG194(*zntA*::*cat*), where the proteins are out-of-frame with the His tag at the carboxy terminus. The absence of the His tag was confirmed by Western blotting using anti-His-tag antibody. The purification protocol for the non-His-tagged proteins has been described recently and takes advantage of the intrinsic metal-binding affinity of the proteins as long as at least one metal-binding site is left intact (*18*). The membranes were solubilized with dodecyl maltoside, and the extract was incubated for 30 min at 4 °C with TALON metal-affinity resin (BD Biosciences), preequilibrated in buffer containing 0.5 mM DDM.[1] The resin was loaded on a column and washed sequentially with the same buffer containing increasing concentrations of imidazole and finally eluted with buffer containing 300 mM imidazole. The protein-containing fractions were concentrated and stored at −70 °C in 25 mM Tris, pH 7.0, containing 100 mM sucrose, 50 mM KCl, 1 mM phenylmethanesulfonyl fluoride, and 0.5 mM DDM. The purity of the proteins was checked by sodium dodecyl sulfate−polyacrylamide gel electrophoresis and found to be >99%.

ATP Hydrolysis and Acyl Phosphate Formation Activity Assays. The metal ion-dependent ATPase activity was determined using a coupled assay with pyruvate kinase and lactate dehydrogenase as described before (*33*). When thiolates were present in the assay medium, the thiolate form of cysteine was added at a soft-metal ion:thiolate ratio of 1:1. Protein concentrations were determined using the bicinchoninic acid reagent (Sigma) with bovine serum albumin as standard.

Phosphorylation of the purified proteins with [γ-^{32}P]ATP was carried out as described earlier with the following modifications (*35*); 10 μg of purified protein, pretreated with 1 mM DTT, was added to 100 μL of reaction mixture containing 50 mM Tris, pH 7.0, 0.1% asolectin, 10% glycerol, and 0.2% Triton X-100 and incubated at 37 °C for 5 min. The appropriate metal salt solution (50 μM) was then added and the reaction incubated for another 10 min. The reaction was then initiated with ~9 μM $MgCl_2$ and 10 μM [γ-^{32}P]ATP. After 20 s at 37 °C, the reaction was stopped with 500 μL of 10% ice-cold TCA containing 1 mM NaH_2PO_4 and 1 mM ATP. The samples were incubated on ice for 10 min and then centrifuged for 10 min. The pellet was washed four times with 10% ice-cold TCA, 1 mM NaH_2PO_4, and 1 mM ATP followed by resuspension in acidic buffer (25 mM H_3PO_4, pH 2.4, 5% SDS) overnight. Blank samples were obtained by adding stop solution before the addition of [γ-^{32}P]ATP. Aliquots were used for scintillation counting.

Phosphorylation with [^{32}P]P_i was carried out with purified proteins (10 μg) pretreated with 2 mM DTT. The proteins were incubated in 100 μL of 50 mM BisTris, pH 7.0, containing 25% dimethyl sulfoxide, 0.2% Triton X-100, and 0.1% asolectin at 37 °C for 5 min, followed by the addition of either water or 30 μM metal salt solution. Following a further incubation for 10 min, the reaction was initiated with 9 mM $MgCl_2$ and 20 μM [^{32}P]P_i. After 10 min, the reaction was stopped with 500 μL of 10% ice-cold TCA containing 1 mM NaH_2PO_4, incubated on ice for 10 min, and centrifuged for 10 min in a microcentrifuge. The pellet was washed three additional times with 10% ice-cold TCA containing 1 mM NaH_2PO_4 and resuspended in 100 μL of 25 mM H_3PO_4, pH 2.4, containing 5% SDS overnight at room temperature. Aliquots were directly counted in a scintillation counter.

Relative Affinity of wtZntA and the Asp714 Mutants for Metal Using Mag-fura-2. The protocol followed for titration using metal indicators was described earlier (*18*, *23*). Extraneous metal ions were removed from the buffers by passing over a Chelex 100 column; buffers were deoxygenated and equilibrated with argon prior to use. Metal-free, reduced protein was prepared by treating 1−2 mg of protein with 2 mM DTT and 5 mM EDTA at 4 °C for 1 h. DTT and EDTA were removed by passage through two consecutive Sephadex G-25 columns. The reduced protein was stored under anaerobic condition and used within 1−2 h. The reduced state of the protein was confirmed by measuring available free cysteines using a standard titration with 5,5′-dithiobis(2-nitrobenzoic acid) (DTNB) (*36*). For competition titration with mag-fura-2, different aliquots of zinc chloride, lead acetate, or cadmium acetate were added using a gastight syringe to 10−20 μM apoprotein and mag-fura-2 (Molecular Probes) in 10 mM BisTris, pH 7.0, in a sealed cuvette under argon. The absorbance maximum of metal-free mag-fura-2 (ϵ = 29900 M^{-1} cm^{-1} at 366 nm) shifts to 325 nm in the metal-bound form (*37*). The stoichiometry and binding affinity of metal ions for the purified proteins were determined by monitoring the absorbance change at 366 nm. The affinity of the different metals for the buffer, BisTris, was taken into account for the calculation (*38*).

Metal-Binding Stoichiometry of the Asp714 Mutants by ICP-MS. Purified, reduced proteins in 10 mM BisTris, pH 7.0, containing 0.5 mM DDM were prepared as described above. They were then incubated with 3-fold excess molar concentrations of different metal salt solutions for 1 h at 4 °C. Unbound metal salts were removed by repeated cycles of dilution and concentration. Control apoprotein samples

[1] Abbreviations: DDM, *n*-dodecyl β-D-maltoside; DTNB, 5,5′-dithiobis(2-nitrobenzoic acid); EDTA, ethylenediaminetetraacetic acid; SDS−PAGE, sodium dodecyl sulfate−polyacrylamide gel electrophoresis.

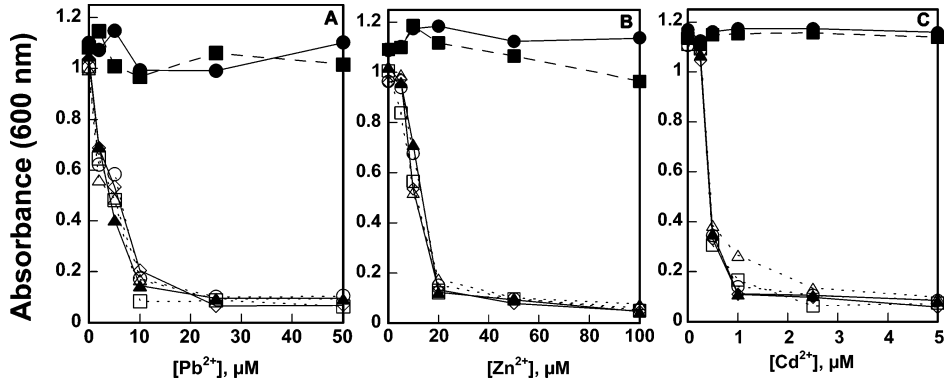

FIGURE 2: Resistance to Pb^{2+}, Zn^{2+}, and Cd^{2+} salts by the wild-type strain LMG194 (solid circles), the *zntA*-deleted strain LMG194-(*zntA*::*cat*) (open triangles), and the deleted strain transformed with plasmids containing *wt*ZntA (solid squares), D714A (open squares), D714H (solid triangles), D714E (open diamonds), and D714P (open circles). Cells were grown at 37 °C in a low-phosphate medium in the absence and presence of different concentrations of (A) lead acetate, (B) zinc chloride, and (C) cadmium chloride. Cell growth was monitored after 24 h by measuring the absorbance at 600 nm.

were subjected to the same treatment. The protein samples were digested with concentrated nitric acid, and their metal content was determined by ICP-MS measurements as described earlier (*19*).

RESULTS

Resistance Profile of the Asp714 Mutants to Growth in the Presence of Pb^{2+}, Zn^{2+}, and Cd^{2+}. ZntA confers resistance to wild-type *E. coli* strains against toxic levels of specifically Pb^{2+}, Cd^{2+}, and Zn^{2+} in the growth medium. The wild-type strain, LMG194, grows well in medium containing toxic levels of these metal salts, but a *zntA*-deleted strain, LMG194(*zntA*::*cat*), is unable to grow, even after an extended period of 24−30 h. However, a plasmid containing a copy of the *wtzntA* gene can complement the defect of the deletion strain (*23*). The Asp714 mutants were tested for their in vivo activity by transforming plasmids bearing them in strain LMG194(*zntA::cat*). None of the mutants, D714A, D714E, D714H, or D714P, were able to confer resistance to Pb^{2+}, Zn^{2+}, and Cd^{2+} salts (Figure 2). The strains containing the mutant genes were unable to grow well even after 30 h; they behaved exactly like the deleted strain, LMG194 (*zntA::cat*). Thus, a single change at Asp714, including the conservative D714E, completely abolished any growth in vivo.

ATPase Activity of the Asp714 Mutants. *wt*ZntA shows ATP hydrolysis activity that is stimulated by Pb^{2+}, Zn^{2+}, or Cd^{2+} salts, with the highest activity obtained with Pb^{2+} (*33*). Three other divalent metal ions, Cu^{2+}, Ni^{2+}, and Co^{2+}, are extremely weak substrates of *wt*ZntA; we have shown previously that these metal ions are capable of forming the acyl phosphate intermediate with ATP, which can be chased by cold ATP (*35*). Thus, this indirect assay indicates that they are capable of hydrolyzing ATP at low rates. No significant activity above background levels was obtained with D714E, D714H, D714A, and D714P, with Pb^{2+}, Zn^{2+}, Cd^{2+}, Cu^{2+}, Ni^{2+}, and Co^{2+}. Thiolates of cysteine or glutathione have been shown earlier to increase the ATPase activity of *wt*ZntA 4−8-fold (*33*). It is possible that the metal thiolate complex is a better substrate; in vivo, metal ions are expected to be present as complexes of small molecule chelators such as cysteine or glutathione. In the presence of metal ions and the thiolate form of cysteine present at a ratio of 1:1, the activities obtained with *wt*ZntA at 37 °C are ∼2500, 800, and 1000 nmol/(mg·min) for Pb^{2+}, Zn^{2+}, and Cd^{2+}, respectively (*25*). Of the four Asp714 mutants, D714A and D714P did not show any activity even in the presence of thiolates. Very low levels of activity were observed with D714E and D714H in the presence of the thiolate form of cysteine. The values obtained for D714E were ∼ 50, 40, and 25 nmol/(mg·min) for Pb^{2+}, Zn^{2+}, and Cd^{2+}, respectively; the values for D714H were ∼30 and 20 nmol/(mg·min) for Zn^{2+} and Cd^{2+}, respectively; D714H showed no activity with Pb^{2+} in the presence of thiolates. These results are consistent with those obtained from metal-binding experiments shown below.

Scheme 1

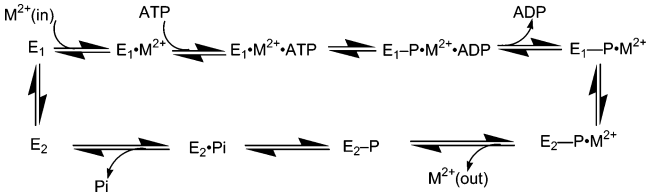

Acyl Phosphate Intermediate Formation for the Asp714 Mutants with [γ-^{32}P]ATP. In common with other P-type ATPases, *wt*ZntA forms an acyl phosphate intermediate in the forward direction with ATP; formation of the intermediate requires prior binding of metal ions (Scheme 1) (*35*, *39*). Though *wt*ZntA has detectable ATP hydrolysis activity only with Pb^{2+}, Zn^{2+}, and Cd^{2+}, it is able to form the acyl phosphate intermediate with Co^{2+}, Ni^{2+}, and Cu^{2+} as well, but not with Ag^{+} or Cu^{+} (*35*). Steady-state levels of the acyl phosphate intermediate are highest with Cd^{2+}, followed by Zn^{2+}, Pb^{2+}, Cu^{2+}, Ni^{2+}, and Co^{2+}. The Asp714 mutants were tested for their ability to form the acyl phosphate intermediate with ATP in the presence of Pb^{2+}, Zn^{2+}, Cd^{2+}, Co^{2+}, Ni^{2+}, and Cu^{2+}. None of the mutant proteins were able to generate any significant amount of acyl phosphate for any of the six metal ions above background levels (Figure 3).

Acyl Phosphate Intermediate Formation for ZntA and the Asp714 Mutants with [^{32}]P_i. P-type ATPases can be phosphorylated to form the acyl phosphate intermediate in the reverse direction with inorganic phosphate, when the protein is in the E_2 conformation (Scheme 1). Since the protein has weak affinity for metal ions in the E_2 conformation, phosphorylation by inorganic phosphate occurs in the absence of bound metal ions. However, binding of metal ions shifts the equilibrium to the E_1 conformation and decreases the

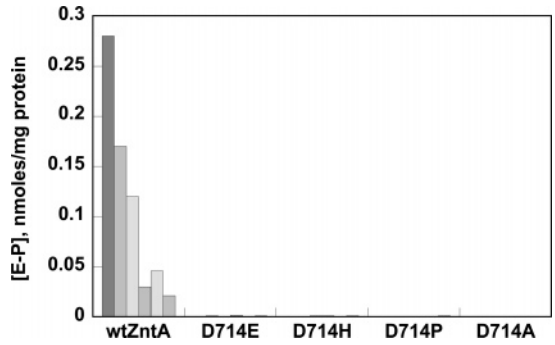

FIGURE 3: Steady-state levels of acyl phosphate formation with purified *wt*ZntA and the Asp714 mutants using [γ-^{32}P]ATP in the absence and presence of different metal salt solutions (50 μM). For each protein, the bars, in order from left to right, represent the results obtained with Cd^{2+}, Zn^{2+}, Pb^{2+}, Co^{2+}, Cu^{2+}, and Ni^{2+}. The background obtained when no metal ions were present in the assay medium has been subtracted. Reactions were carried out for 20 s at 37 °C.

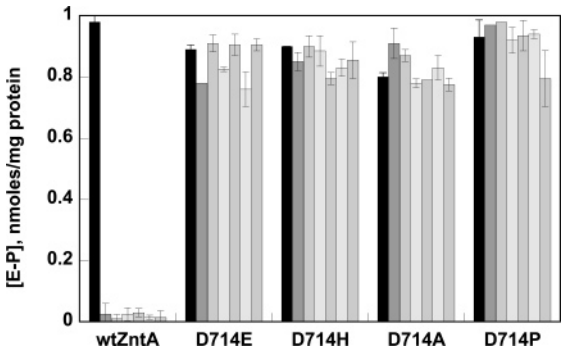

FIGURE 4: Acyl phosphate formation with purified *wt*ZntA and the Asp714 mutants using ^{32}P-labeled inorganic phosphate in the absence and presence of different metal salt solutions (30 μM). For each protein, the bars represent the results obtained with no metal (black bars) and, in order from left to right, Cd^{2+}, Zn^{2+}, Pb^{2+}, Co^{2+}, Cu^{2+}, and Ni^{2+}. Reactions were carried out for 10 min at 37 °C.

amount of acyl phosphate formed in the reverse direction. As shown in Figure 4, *wt*ZntA is phosphorylated by inorganic phosphate in the absence of metal ions; in the presence of Pb^{2+}, Zn^{2+}, Cd^{2+}, Cu^{2+}, Co^{2+}, and Ni^{2+}, there is no acyl phosphate intermediate formed.

To eliminate the possibility that the inactivity of the Asp714 mutants was simply due to incorrectly folded proteins, they were tested for their ability to form the acyl phosphate intermediate with inorganic phosphate. All four mutants, D714E, D714H, D714A, and D714P, were competent in forming the intermediate with [^{32}P]P_i in the absence of metal ions; the steady-state levels of intermediate generated were similar to that by *wt*ZntA, ~1 nmol/mg of protein (Figure 4). Thus, the overall inactivity of the mutant proteins was not due to problems in protein folding or membrane insertion since they are able to catalyze a partial reaction in the reverse direction as well as *wt*ZntA. It should be noted, however, that unlike *wt*ZntA the steady-state levels of the intermediate did not decrease upon addition of any of the six metal ions for the mutant proteins. These data indicate that, for the mutant proteins, the step involving metal ion binding had been compromised as compared to *wt*ZntA.

Affinity of Zn^{2+}, Pb^{2+}, and Cd^{2+} for the Transmembrane Site in the Asp714 Mutants Using Mag-fura-2. In earlier work, ICP-MS measurements revealed that *wt*ZntA has two high-affinity metal-binding sites, one in the hydrophilic

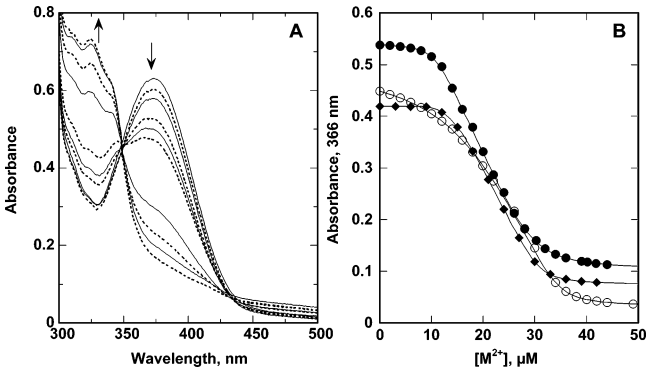

FIGURE 5: (A) Representative spectra obtained during titration of a mixture of ~21 μM mag-fura-2 and ~16 μM *wt*ZntA with increasing concentrations of zinc chloride in 10 mM BisTris, pH 7.0 and 20 °C. (B) Plot of the absorbance change at 366 nm when increasing concentrations of metal salt solutions were added to mag-fura-2 and *wt*ZntA in 10 mM BisTris, pH 7.0 and 20 °C. Data were fitted to eqs 1−4. Solid circles, Pb^{2+}; open circles, Zn^{2+}; solid diamonds, Cd^{2+}. The concentrations of *wt*ZntA used were ~10, 10, and 12 μM for Pb^{2+}, Zn^{2+}, and Cd^{2+}, respectively; the corresponding values of mag-fura-2 were ~18, 15, and 14 μM.

N-terminal domain and another in the transmembrane domain (*18*, *23*). The cysteines of the CPC motif in transmembrane helix 6 supply ligands to the second metal site (Figure 1) (*18*). To establish whether Asp714 also acts as a ligand to the transmembrane metal site, the binding affinity of each of the Asp714 mutants for metal ions was measured by competition titration with a metal ion indicator. The experiments were performed with purified, reduced proteins. The number of free cysteines was measured by the DTNB assay for the reduced proteins to ensure that, following reduction of the proteins and removal of excess reducing reagent, they remained fully reduced during the course of the metal-binding experiments. Reduced *wt*ZntA as well as the Asp714 mutants had six and nine free cysteines under nondenaturing and denaturing conditions, respectively, indicating that the proteins remained fully reduced during the metal-binding experiments.

The affinity of the two metal-binding sites was determined for reduced *wt*ZntA and the Asp714 mutants for the metal ions, Zn^{2+}, Pb^{2+}, and Cd^{2+}, by titration with mag-fura-2. This indicator forms a 1:1 complex with divalent metal ions; the metal-free form of mag-fura-2 has an absorbance maximum at 366 nm, which changes to ~325 nm when metal is bound. Under the experimental conditions, a mixture of mag-fura-2 and reduced protein was titrated with aliquots of metal salt. The absorbance at 366 nm decreased as increasing amounts of metal ion were bound to the indicator in competition with the protein. Figure 5A shows a typical titration of Zn^{2+} with mag-fura-2 and *wt*ZntA. Figure 5B shows the decrease in absorbance at 366 nm versus Pb^{2+}, Zn^{2+}, and Cd^{2+} concentration, obtained with *wt*ZntA for similar titration with all three metal salts. The data were fitted simultaneously to eqs 1−4 using the software Dynafit (*40*):

$$E + M^{2+} \overset{K_{1E}}{\longleftrightarrow} E{\cdot}M^{2+} \quad (1)$$

$$E{\cdot}M^{2+} + M^{2+} \overset{K_{2E}}{\longleftrightarrow} E{\cdot}(M^{2+})_2 \quad (2)$$

$$I + M^{2+} \overset{K_{I}}{\longleftrightarrow} I{\cdot}M^{2+} \quad (3)$$

$$B + M^{2+} \overset{K_{B}}{\longleftrightarrow} B{\cdot}M^{2+} \quad (4)$$

Table 1: Association Constants for Binding of Different Metal Ions to *wt*ZntA and the Asp714 Mutant Proteins Using Competition Titration with Mag-fura-2[a]

	lead	zinc	cadmium
*wt*ZntA	$(1.3 \pm 0.1) \times 10^9$	$(1.1 \pm 0.1) \times 10^8$	$(1.3 \pm 0.1) \times 10^8$
	$(4.5 \pm 0.1) \times 10^9$	$(5.0 \pm 0.1) \times 10^8$	$(5.0 \pm 0.1) \times 10^8$
D714E	$(1.3 \pm 0.1) \times 10^9$	$(1.1 \pm 0.1) \times 10^8$	$(1.3 \pm 0.03) \times 10^8$
	$(4.6 \pm 0.04) \times 10^9$	$(5.0 \pm 0.4) \times 10^8$	$(5.0 \pm 0.4) \times 10^8$
D714H	$(1.3 \pm 0.01) \times 10^9$	$(1.3 \pm 0.1) \times 10^8$	$(1.3 \pm 0.03) \times 10^8$
		$(1.0 \pm 0.2) \times 10^8$	$(5.0 \pm 0.02) \times 10^8$
D714A[b]	$(2.6 \pm 0.01) \times 10^9$	$(2.6 \pm 0.1) \times 10^8$	$(1.1 \pm 0.01) \times 10^8$
D714P[b]	$(1.3 \pm 0.1) \times 10^9$	$(1.3 \pm 0.01) \times 10^8$	$(1.1 \pm 0.01) \times 10^8$

[a] Units are in M^{-1}. Protein samples were prepared as described in Experimental Procedures. Data were fitted using Dynafit (*40*) with the assumption of two binding sites, except for D714A and D714P, where only one binding site was assumed in the fit. The reported values are averages of independent titrations with two different protein preparations. [b] Fitting the data using a two binding site model yielded an unrealistically low value for the second association constant. This was also true for the binding of Pb^{2+} to D714H.

Equations 1 and 2 describe the association constants (K_{1E} and K_{2E}) of two metal ions (M) with *wt*ZntA (E). Equation 3 describes the association constant (K_I) of mag-fura-2 (I) with metal ion while eq 4 describes the association constant (K_B) of the buffer, BisTris (B), with metal ion. The value of the association constant, K_I, of mag-fura-2 for Zn^{2+}, Cd^{2+}, and Pb^{2+} was previously determined in 10 mM BisTris, pH 7.0 at 20 °C (*18*). These values of K_I for Zn^{2+}, Cd^{2+}, and Pb^{2+} were 5×10^7, 3×10^7, and 3×10^8 M^{-1}, respectively; the value for Zn^{2+} has been reported in the literature to be 5×10^7 M^{-1} (*41*). For the fits shown in Figure 5B, these values were used either directly in eq 3 or K_I was treated as a variable during the data fitting. When K_I was a variable, the values obtained for it were within 1−4-fold of the experimentally determined values. The buffer used in these experiments was BisTris, which forms a stable and soluble complex with Pb^{2+} and prevents formation of insoluble lead compounds. The association constant, K_B, for the binding of different metal ions to BisTris is known; the values for Pb^{2+}, Zn^{2+}, and Cd^{2+} are 2.1×10^4, 240, and 300 M^{-1}, respectively (*38*). These values were used in the data fitting. The excellent fit of the data in Figure 5B indicates that, under equilibrium conditions, *wt*ZntA has two tight metal-binding sites as described by eqs 1 and 2. The data could not be fitted to a model that assumes a single binding site on the protein. Table 1 shows the association constants obtained for the two metal-binding sites in *wt*ZntA.

The number of metal-binding sites and their affinity for the Asp714 mutants were determined by similar titration experiments with mag-fura-2. The results are shown in Figure 6 for D714E, D714H, D714A, and D714P. The titration data for D714E for Pb^{2+}, Zn^{2+}, and Cd^{2+} could be fitted well to eqs 1−4, indicating that this mutant has two binding sites for all three metal ions. The association constants for the two sites are similar to those obtained for *wt*ZntA for all three cations (Table 1). However, for D714A and D714P, the titration data (Figure 6C,D) for the three metal ions were best fitted to eqs 1, 3, and 4, which describe a single metal-binding site on the protein. The values of K_{1E} obtained for the binding of the three metal ions to these two mutants were also similar, within error, to those of *wt*ZntA.

D714H proved to be especially interesting (Figure 6B). Binding of Pb^{2+} to this mutant resembled that of D714A and D714P, with only one high-affinity metal-binding site present. Data were fitted to eqs 1, 3, and 4. Attempting to fit the data to eqs 1−4 resulted in a second affinity constant with a value in the molar range, indicating that a second specific metal-binding site is no longer present. On the other hand, binding of Zn^{2+} and Cd^{2+} to D714H resembled that of *wt*ZntA and D714E, in that this mutant bound two of these metal ions with high affinity. The data were fitted to eqs 1−4, similar to *wt*ZntA and D714E, and metal affinities obtained were similar to those of *wt*ZntA and D714E (Table 1).

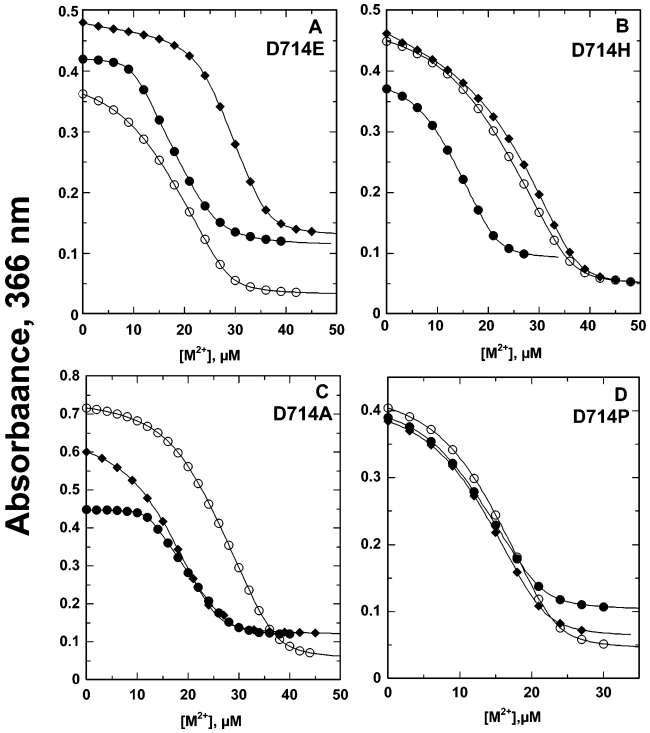

FIGURE 6: Plot of the absorbance changes at 366 nm when increasing concentrations of metal salt solutions were added to mag-fura-2 and the Asp714 mutants in 10 mM BisTris, pH 7.0 and 20 °C. (A) D714E; (B) D714H; (C) D714A; (D) D714P. Data were fitted as discussed in the Results section. Solid circles, Pb^{2+}; open circles, Zn^{2+}; solid diamonds, Cd^{2+}. The protein and indicator concentrations used were as follows: (A) ∼11, 11, and 10 μM D714E for Pb^{2+}, Zn^{2+}, and Cd^{2+}, respectively; the corresponding values of mag-fura-2 were ∼14, 12, and 16 μM. (B) ∼10 μM D714H for all three metal ions; the values of mag-fura-2 were ∼12, 15, and 15 μM for Pb^{2+}, Zn^{2+}, and Cd^{2+}, respectively. (C) ∼15, 15, and 11 μM D714A for Pb^{2+}, Zn^{2+}, and Cd^{2+}, respectively; the corresponding values of mag-fura-2 were ∼15, 24, and 20 μM. (D) ∼9, 12, and 9 μM D714P for Pb^{2+}, Zn^{2+}, and Cd^{2+}, respectively; the corresponding values of mag-fura-2 were ∼13 μM for all three metal ions.

Table 2: Stoichiometry of Metal Bound to *wt*ZntA, D714E, D714H, D714A, and D714P Using ICP-MS[a]

	lead	zinc	cadmium
*wt*ZntA[b]	1.8 ± 0.1	2.2 ± 0.0	1.9 ± 0.0
D714E	2.0 ± 0.2	2.0 ± 0.4	1.8 ± 0.2
D714H	1.0 ± 0.01	1.8 ± 0.2	1.8 ± 0.2
D714A	1.1 ± 0.1	1.1 ± 0.1	1.1 ± 0.1
D714P	1.0 ± 0.1	0.9 ± 0.2	1.0 ± 0.1

[a] Samples were prepared as described in Experimental Procedures. [b] From ref *18*.

To support the results obtained with the mag-fura-2 titration, the stoichiometry of metal ions bound to the Asp714

mutants was also determined by ICP-MS measurements. Values obtained for D714A and D714P were ~1 for all three metals, lead, zinc, and cadmium, as also for D714H with lead (Table 2). The values for D714E for all three metals, and for D714H with cadmium and zinc, were 1.8−2.0.

DISCUSSION

Despite a high level of overall sequence homology, P_{1B}-type ATPases can be divided into subgroups that are specific for different groups of soft metal ions (*26*). This specificity is likely to arise from highly conserved metal-binding sites for each subgroup. The metal-binding site(s) in the N-terminal domain of P_{1B}-type ATPases has (have) different conserved sequences depending on the metal ions transported. Pumps transporting Cu^+/Ag^+ or $Pb^{2+}/Zn^{2+}/Cd^{2+}$ contain the CXXC metal-binding motif. The subgroup transporting Pb^{2+}, Zn^{2+}, and Cd^{2+} has a conserved acidic Asp/Glu metal ligand in addition to the CXXC motif; this Asp/Glu can be part of the GX**D**CXXC motif as in ZntA or be located elsewhere as in CadA from *Listeria monocytogene*s and homologues where a conserved Glu residue is located in the loop between the α2 and *β*2 segments of the structure, apart from the GXXCXXC motif (*42*). Pumps displaying the highest activity with Pb^{2+} also contain a separate distinct Cys/Asp-containing motif at the N-terminus in addition to the GXDCXXC motif (*23*). The metal site in the N-terminal domain of Cu^{2+}-ATPases is histidine-rich (*14*) while Co^{2+}-transporting ATPases appear to lack a metal-binding N-terminal domain (*10*).

Such different groups of conserved metal-binding residues are likely to exist for the transmembrane metal-binding site in P_{1B}-type ATPases displaying different metal specificity as well. A sequence alignment of P_{1B}-type ATPases confirms this to be the case, particularly for residues in transmembrane helices 6−8 of these pumps (*26*). In the middle of transmembrane helix 6, all P_{1B}-type ATPases contain the distinctive (C,S,T)P(C,H) motif. For Cu^+/Ag^+- or $Pb^{2+}/Zn^{2+}/Cd^{2+}$-transporting pumps, the motif is CPC, while for the Cu^{2+} pumps, it is CPH, and for the Co^{2+}-ATPases, it is probably (S,T)PC. The cysteines flanking the proline supply ligands to the metal ion in ZntA, since metal binding to the transmembrane site is eliminated when the cysteines are altered to alanine by site-specific mutagenesis (*18*). In this work, our goal was to examine additional transmembrane metal-binding residues in the ZntA subgroup of P_{1B}-type ATPases that would distinguish them from the Cu^+/Ag^+ subgroup. Given that an acidic residue, an aspartate, is strictly conserved in the center of transmembrane helix 8 for only the ZntA subgroup, it was likely that this residue supplied ligands to the metal ion in the transmembrane site in addition to the two cysteines of the CPC motif.

Four different mutants were characterized at residue 714. The conservative mutation D714E was designed to test whether an acidic group at this position was sufficient to retain high metal-binding affinity as well as activity. In D714H, the imidazole side chain of histidine replacing the carboxylate oxygens of the aspartate side chain was also be expected to supply ligands to the metal ion; additionally, sequence alignments show that the Co^{2+}-ATPases contain a histidine at the position corresponding to Asp714. The D714A mutation was chosen to eliminate any possibility of the side chain at residue 714 acting as a metal ligand. The D714P mutant was characterized because Cu^+-transporting ATPases have a conserved proline at the residue corresponding to Asp714. Metal-binding studies showed that D714A and D714P lost the ability to bind a metal ion at the transmembrane site, though the N-terminal site was still able to bind a metal ion in these mutants. The conservative mutation D714E could bind all three substrate metal ions with affinity very similar to that of *wt*ZntA. In D714H, the nitrogen of the imidazole side chain could coordinate Zn^{2+} and Cd^{2+}, but not Pb^{2+}; this is likely because Pb^{2+}, a large and thiophilic metal ion, usually does not prefer to coordinate with nitrogen-containing ligands. It is also possible that the binding geometry of Pb^{2+} at the transmembrane site is somewhat different from that of Zn^{2+} and Cd^{2+}, as is true for the N-terminal site in ZntA (*23*). These results clearly show that Asp714 is a metal-binding ligand in the ZntA subgroup of P_{1B}-ATPases; it may supply one or two oxygen ligands to the metal ion through its carboxylate oxygens. Together with Cys392 and Cys394, Asp714 is part of the metal-binding site in the transmembrane domain. Whether additional ligands also exist is not clear at this time, but it should be pointed out that Zn^{2+} binds to the N-terminal site in ZntA by coordinating to two cysteines and an aspartate residue (*20*). However, clearly, cysteines at positions 392 and 394 or conservative substitutions such as serine or histidine are transmembrane metal-binding ligands common to all P_{1B}-ATPase subgroups (Figure 1), whereas Asp714 is unique to ZntA homologues and is required for binding the substrate metal ions of this subgroup.

None of the four mutations at Asp714 showed any resistance activity in vivo. It is possible that the absence of in vivo resistance activity is due to decreased stability of the mutant proteins; however, this is unlikely since they appeared to have stability comparable to *wt*ZntA in vitro. It should be noted that the level of expression of the mutant proteins was similar to that of *wt*ZntA. Since they could catalyze the partial reverse reaction of forming the E_2P intermediate with inorganic phosphate as competently as *wt*ZntA, none of the substitutions at Asp714 lead to any major structural changes in the transporter, including the potentially helix destabilizing substitution, D714P. For D714A and D714P, the lack of resistance activity, as well as in vitro ATPase activity, is expected since they are unable to bind a metal ion at the transmembrane site. However, D714E and D714H, which were capable of binding all or some of the substrate metal ions with high affinity, showed no resistance activity, 25−50-fold lower ATPase activity compared to *wt*ZntA, and were unable to form the E_1P intermediate with ATP in an in vitro assay carried out without any thiolates in the medium. In *wt*ZntA, metal binding induces ATP to be hydrolyzed to ADP and form the acyl phosphate intermediate (Scheme 1). The surprising observation in this work suggests that though D714E and D714H can bind metal ions with high affinity, the bound metals are unable to induce changes in the protein structure that lead to efficient ATP hydrolysis and formation of the acyl phosphate intermediate. This supports an earlier conclusion that optimal metal-binding geometry, and not metal-binding affinity, leads to metal selectivity in ZntA (*18*). It is likely that, in the ZntA subgroup, Asp714, Cys392, and Cys 394 are optimally positioned such that the three substrate metal

ions, Pb^{2+}, Zn^{2+}, and Cd^{2+}, can bind and induce the conformational changes essential for rapid catalysis. Even with one additional methylene group in the side chain for D714E, catalytic competence is lost. Complete loss in activity was observed for the D800E and D800N mutants in SERCA1 (*27*). Interestingly, no ATPase or E1 acyl phosphate formation activity was obtained for the D714H mutant with Co^{2+}, though in Co^{2+}-ATPases the residue corresponding to Asp714 is a histidine. This implies that optimal metal-binding geometry that leads to activity may be difficult to attain by simply changing the primary ligands. It is also possible that, in the Co^{2+}-ATPases, the corresponding histidine is not a metal ligand or that it is crucial to alter the CPC motif in transmembrane domain 6 to the (S,T)PC motif found in Co^{2+}-ATPases.

SERCA1 binds two Ca^{2+} ions in the membrane domain with 7-coordinate geometry, with Asp800 coordinating both Ca^{2+} sites (*32*). ZntA binds only one metal ion in the membrane domain, with Asp714 supplying one or two ligands to the metal ion. Thus, though the number and possibly geometry of bound metal ions in the membrane domain of these two distantly related P-type ATPases are different, a crucial metal-binding residue has been conserved in both the ZntA subgroup of P_{1B}-type ATPases and P_2-type ATPases such as SERCA1.

In previous work, we measured the binding affinity of the two metal sites in ZntA individually in isolated fragments containing only one functional metal-binding site. The N-terminal site was characterized in the isolated N-terminal domain of ZntA (*23*); the transmembrane site was characterized in mutants in which the N-terminal domain was deleted altogether or in which the N-terminal site was knocked out by site-specific mutagenesis (*18*). The affinity obtained for the individual sites earlier is very similar to those reported here for *wt*ZntA in which both sites can bind metal ions simultaneously. This demonstrates that the metal affinity of the two sites does not change when a second functional site is present. However, it is possible that, during the actual reaction cycle, the N-terminal site may exert a negative cooperative effect on the transmembrane site in the E2 state, thereby inducing the metal ion to be released. In all four Asp714 mutants, the affinity of the N-terminal site for metal ions remained similar to that of *wt*ZntA, showing that Asp714, a ligand to the transmembrane site, has no direct interaction with the N-terminal site in the absence of ATP.

Conclusions. ZntA and its homologues have a strictly conserved Asp714 in the eighth transmembrane domain that is not present in any other subgroup of P_{1B}-type ATPases. By characterizing four different mutants at Asp714 and measuring their metal-binding affinity, we show that this residue is a ligand for the metal ion in the transmembrane site. Thus, Asp714 is one of the residues that determine metal specificity in ZntA homologues. All substitutions at this position, including the conservative D714E, resulted in complete loss of in vivo metal resistance activity and greatly decreased or no ATP hydrolysis activity. All of the mutants were competent in catalyzing acyl phosphate formation in the reverse direction. Additionally, mutants such as D714E and D714H retained the ability to bind metal ions with high affinity, but lost overall activity. This suggests that binding metal ions with high affinity does not correlate with high activity. The affinities of the two metal-binding sites in *wt*ZntA determined in this study are similar to values reported previously for the isolated sites, suggesting that, in the E1 state, the two sites in ZntA do not display cooperativity in metal binding.

ACKNOWLEDGMENT

We thank Dr. Ann J. Stemmler for help with the ICP-MS experiments.

REFERENCES

1. Axelson, K. B., and Palmgren, M. G. (1998) Evolution of substrate specificities in the P-type ATPase superfamily, *J. Mol. Evol. 46*, 84−101.
2. Lutsenko, S., and Kaplan, J. H. (1995) Organization of P-type ATPases: Significance of structural diversity, *Biochemistry 34*, 15607−15613.
3. Nucifora, G., Chu, L., Misra, T. K., and Silver, S. (1989) Cadmium resistance from *Staphylococcus aureus* plasmid pI258 cadA gene results from a cadmium-efflux ATPase, *Proc. Natl. Acad. U.S.A. 86*, 3544−3548.
4. Mercer, J. F., Livingston, J., Hall, B., Paynter, J. A., Begy, C., Chandrasekharappa, S., Lockhart, P., Grimes, A., Bhave, M., Siemieniak, D., et al. (1993) Isolation of a partial candidate gene for Menkes disease by positional cloning, *Nat. Genet. 3*, 20−25.
5. Vulpe, C., Levinson, B., Whitney, S., Packman, S., and Gitschier, J. (1993) Isolation of a candidate gene for Menkes disease and evidence that it encodes a copper-transporting ATPase, *Nat. Genet. 3*, 7−13.
6. Bull, P. C., Thomas, G. R., Rommens, J. M., Forbes, J. R., and Cox, D. W. (1993) The Wilson disease gene is a putative copper transporting P-type ATPase similar to the Menkes gene, *Nat. Genet. 5*, 327−337.
7. Odermatt, A., Suter, H., Krapf, R., and Solioz, M. (1993) Primary structures of two P-type ATPases Involved in copper resistance in *Enterococcus hirae*, *J. Biol. Chem. 268*, 12775−12779.
8. Rensing C., Mitra B., and Rosen B. P. (1997) The *znt*A gene of *Escherichia coli* encodes a Zn^{2+}-translocating P-type ATPase, *Proc. Natl. Acad. Sci. U.S.A. 94*, 14326−14331.
9. Rensing, C., Sun, Y., Mitra, B., and Rosen, B. P. (1998) Pb^{2+}-translocating P-type ATPases, *J. Biol. Chem. 273*, 32614−32617.
10. Rutherford, J. C., Cavet, J. S., and Robinson, N. (1999) Cobalt-dependent transcriptional switching by a dual-effector MerR-like protein regulates a cobalt-exporting variant CPx-type ATPase, *J. Biol. Chem. 274*, 25827−2832.
11. Gupta, A., Matsui, K., Lo, J. F., and Silver, S. (1999) Molecular basis for resistance to silver cations in *Salmonella*, *Nat. Med. 5*, 183−188.
12. Mandal, A. K., Cheung, W. D., and Arguello, J. M. (2002) Characterization of a thermophilic P-type Ag^+/Cu^+-ATPase from the extremophile *Archaeoglobus fulgidus*, *J. Biol. Chem. 277*, 7201−7208.
13. Rensing, C., Fan, B., Sharma, R., Mitra, B., and Rosen, B. P. (2000) CopA: an *Escherichia coli* Cu(I)-translocating P-type ATPase, *Proc. Natl. Acad. Sci. U.S.A. 97*, 652−656.
14. Mana-Capelli, S., Mandal, A. K., and Arguello, J. M. (2003) *Archaeoglobus fulgidus* CopB is a thermophilic Cu^{2+}-ATPase: functional role of its histidine-rich-N-terminal metal binding domain, *J. Biol. Chem. 278*, 40534−40541.
15. Fan, B., and Rosen, B. P. (2002) Biochemical characterization of CopA, the *Escherichia coli* Cu(I)-translocating P-type ATPase, *J. Biol. Chem. 277*, 46987−46992.
16. Mandal, A. K., and Arguello, J. M. (2003) Functional roles of metal binding domains of the *Archaeoglobus fulgidus* Cu(+)-ATPase CopA, *Biochemistry 42*, 11040−11047.
17. Bal, N., Wu, C. C., Catty, P., Guillain, F., and Mintz, E. (2003) Cd^{2+} and the N-terminal metal-binding domain protect the putative membranous CPC motif of the Cd^{2+}-ATPase of *Listeria monocytogenes*, *Biochem. J. 369*, 681−685.
18. Liu, J., Dutta, S. J., Stemmler, A. J., and Mitra, B. (2006) Metal-binding affinity of the transmembrane site in ZntA: Implications for metal selectivity, *Biochemistry 45*, 763−772.
19. Gitschier, J., Moffat, B., Reilly, D., Wood, W. I., and Fairbrother, W. J. (1998) Solution structure of the fourth metal-binding domain from the Menkes copper-transporting ATPase, *Nat. Struct. Biol. 5*, 47−54.

20. Banci, L., Bertini, I., Ciofi-Baffoni, S., Finney, L. A., Outten, C. E., and O'Halloran, T. V. (2002) A new zinc-protein coordination site in intracellular metal trafficking: solution structure of the apo and Zn(II) forms of ZntA(46−118), *J. Mol. Biol. 323*, 883−897.
21. Banci, L., Bertini, I., Del Conte, R., D'Onofrio, M., and Rosato, A. (2004) Solution structure and backbone dynamics of the Cu(I) and apo forms of the second metal-binding domain of the Menkes protein ATP7A, *Biochemistry 43*, 3396−33403.
22. Ralle, M., Cooper, M. J., Lutsenko, S., and Blackburn, N. J. (1998) The Menkes disease protein binds copper via novel 2-coordinate Cu^{+}−cysteinates in the N-terminal domain, *J. Am. Chem. Soc. 120*, 13525−13526.
23. Liu, J., Stemmler, A. J., Fatima, J., and Mitra, B. (2005) Metal-binding characteristics of the amino-terminal domain of ZntA: Binding of lead is different compared to cadmium and zinc, *Biochemistry 44*, 5159−5167.
24. Dutta, S. J., Liu, J., and Mitra, B. (2005) Kinetic analysis of metal binding to the amino-terminal domain of ZntA by monitoring metal−thiolate charge-transfer complexes, *Biochemistry 44*, 14268−14274.
25. Mitra, B., and Sharma, R. (2001) The cysteine-rich amino-terminal domain of ZntA, a Pb(II)/Cd(II)/Zn(II)-translocating ATPase from *Escherichia coli*, is not essential for its function, *Biochemistry 40*, 7694−7699.
26. Arguello, J. M. (2003) Identification of ion-selectivity determinants in heavy-metal transport P_{1B}-type ATPases, *J. Membr. Biol. 195*, 93−108.
27. Clarke, D. M., Loo, T. W., and MacLennan, D. H. (1990) Functional consequences of alterations to polar amino acids located in the transmembrane domain of the Ca2(+)-ATPase of sarcoplasmic reticulum, *J. Biol. Chem. 265*, 6262−6267.
28. Rice, W. J., and MacLennan, D. H. (1996) Scanning mutageneis reveals a similar pattern of mutation sensitivity in transmembrane sequences M4, M5, and M6, but not in M8, of the Ca^{2+}-ATPase of sarcoplasmic reticulum (SERCA1a), *J. Biol. Chem. 271*, 31412−31419.
29. Kuntzweiler, T. A, Arguello, J. M., and Lingrel, J. B. (1996) Asp804 and Asp808 in the transmembrane domain of the Na, K-ATPase alpha subunit are cation coordinating residues, *J. Biol. Chem. 271*, 29682−29687.
30. Asano, S., Io, T., Kimura, T., Sakamoto, S., and Takeguchi, N. (2001) Alanine-scanning mutagenesis of the sixth transmembrane segment of gastric H^{+}, K^{+}-ATPase alpha-subunit, *J. Biol. Chem. 276*, 31265−31273.
31. Buch-Pedersen, M. J., Venema, K., Serrano, R., and Palmgren, M. G. (2000) Abolishment of proton pumping and accumulation in the E1P conformational state of a plant plasma membrane H^{+}-ATPase by substitution of a conserved aspartyl residue in transmembrane segment 6, *J. Biol. Chem. 275*, 39167−39173.
32. Toyoshima, C., Nakasako, M., Nomura, H., and Ogawa, H. (2000) Crystal structure of the calcium pump of sarcoplasmic reticulum at 2.6 Å resolution, *Nature 405*, 647−655.
33. Sharma, R., Rensing, C., Rosen, B. P., and Mitra, B. (2000) The ATP hydrolytic activity of purified ZntA, a Pb^{2+}/Cd^{2+}/Zn^{2+}-translocating ATPase from *Escherichia coli*, *J. Biol. Chem. 275*, 3873−3878.
34. Poole, R. K., Williams, H. D., Downie, J. A., and Gibson, F. (1989) Mutations affecting the cytochrome d-containing oxidase complex of *Escherichia coli* K12: Identification and mapping of a fourth locus, cydD, *J. Gen. Microbiol. 135*, 1865−1874.
35. Hou, Z., and Mitra, B. (2003) Characterization of the metal specificity of ZntA from *Escherichia coli* using the acylphosphate intermediate, *J. Biol. Chem. 278*, 28455−28461.
36. Riddles, P. W., Blakeley, R. L., and Zerner, B. (1979) Ellman's reagent: 5,5′-dithiobis(2-nitrobenzoic acid)−a reexamination, *Anal. Biochem. 94*, 75−81.
37. Walkup, G. K., and Imperiali, B. (1997) Fluorescent chemosensors for divalent zinc based on zinc finger domains. Enhanced oxidative stability, metal binding affinity, and structural and functional characterization, *J. Am. Chem. Soc. 119*, 3443−3450.
38. Sigel, H. (1987) Isomeric equilibria in complexes of adenosine 5′-triphosphate with divalent metal ions. Solution structures of $M(ATP)^{2-}$ complexes, *Eur. J. Biochem. 165*, 65−72.
39. Inesi, G. (1985) Mechanism of calcium transport, *Annu. Rev. Physiol. 47*, 573−601.
40. Kuzmic, P. (1996) Program DYNAFIT for the analysis of enzyme kinetic data: Application to HIV proteinase, *Anal. Biochem. 237*, 260−273.
41. Simons T. J. (1993) Measurement of free Zn^{2+} ion concentration with the fluorescent probe mag-fura-2 (furaptra), *J. Biochem. Biophys. Methods 27*, 25−37.
42. Banci, L., Bertini, I., Ciofi-Baffoni, S., Su, X. C., Miras, R., Bal, N., Mintz, E., Catty, P., Shokes, J. E., and Scott, R. A. (2006) Structural basis for metal binding specificity: The N-terminal cadmium binding domain of the P1-type ATPase CadA, *J. Mol. Biol. 356*, 638−650.

BI0523456